Pattern Recognition Letters 30 (2009) 456–459

Contents lists available at ScienceDirect

Pattern Recognition Letters

journal homepage: www.elsevier.com/locate/patrec

Morphological segmentation of binary patterns

Pierre Soille [a,*], Peter Vogt [b]

[a] Spatial Data Infrastructures Unit, Institute for Environment and Sustainability, Joint Research Centre, European Commission, via Fermi 2749, I-21027 Ispra, Italy
[b] Land Management and Natural Hazards Unit, Institute for Environment and Sustainability, Joint Research Centre, European Commission, via Fermi 2749, I-21027 Ispra, Italy

ARTICLE INFO

Article history:
Received 8 May 2008
Received in revised form 27 October 2008
Available online 13 November 2008

Communicated by G. Borgefors

Keywords:
Morphological image analysis
Pattern segmentation
Connectivity

ABSTRACT

This paper presents a method for segmenting binary patterns into seven mutually exclusive categories: core, islet, loop, bridge, perforation, edge, and branch. This is achieved by applying a series of morphological transformations such as erosions, geodesic dilations, reconstruction by dilation, anchored skeletonisation, etc. The proposed method depends on a single parameter only and can be used for characterising binary patterns with emphasis on connections between their parts as measured at varying analysis scales. This is illustrated on two examples related to land cover maps and circuit board defect detection.

1. Introduction

Once a digital image has been segmented and each segment assigned to a given class of objects, binary maps indicating whether each given pixel belongs or not to a specific class can be produced. For example, in remote sensing, the classification of an image into land cover classes leads to binary maps of any specific land cover class. Measurements can then be performed to investigate the shape and size of the spatial patterns occurring in these maps. A wide variety of techniques are available for producing meaningful measurements. For instance, when dealing with patterns resembling to disks of varying size, granulometries reveal the size distribution of these patterns. A series of other morphometric measurements are proposed in (Beisbart et al., 2001). Rather than performing direct measurements on the input pattern, we propose a new approach where the input pattern is segmented into a series of categories revealing information about its size, shape, and connectivity. In addition, this segmentation relies on a size-parameter since the interaction between a given phenomenon related to the mapped object depends on the phenomenon itself. For example, the so-called core category can be viewed as the subset of the pattern that is far enough from its boundary. This naturally leads to a distance based definition using a distance threshold whose value depends on the phenomenon under study.

This paper is organised as follows. The proposed method is detailed in Section 2. Experimental results are provided and discussed in Section 3. Concluding remarks are presented in Section 4.

2. Method

Several methods are already available for segmenting binary patterns. For example, the watershed transformation of the complement of the filtered distance transform can be used for segmenting overlapping blobs (Vincent and Soille, 1991). However, this method assumes that the blobs do not deviate too much from a disk-like shape. Therefore, it cannot be used for segmenting arbitrary patterns. We propose hereafter a simple and general purpose approach relying on a single parameter and leading to the segmentation of arbitrary binary patterns into seven categories: core, islet, loop, bridge, perforation, edge, and branch. All categories are obtained by applying a series of operators originating from mathematical morphology (Serra, 1982). We use the notations and definitions detailed in (Soille, 2003).

Let f be a binary image in the square grid with foreground pixels set to 1 and background pixels set to 0. We use the notion of path connectivity to establish whether a group of foreground (resp. background) pixels is connected or not. To avoid the connectivity paradox of raster grids, we assume that the foreground is 8-connected and therefore the background is 4-connected (or vice versa).

The proposed size dependent characterisation is based on a size-parameter corresponding to a Euclidean distance threshold value. We denote this size-parameter by s. Since the analysis is performed on a raster grid, a size of 1 is equal to the distance separating the centre of two 4-adjacent pixels (i.e. the width of a pixel). The next possible size corresponds to the distance separating

* Corresponding author. Tel.: +39 0332 785 068; fax: +39 0332 789 536.
E-mail address: Pierre.Soille@jrc.it (P. Soille).

0167-8655/$ - see front matter © 2008 Elsevier B.V. All rights reserved.
doi:10.1016/j.patrec.2008.10.015

the centre of two 8-adjacent pixels (i.e. $\sqrt{2}$). In general, the size s is in the form $\sqrt{a^2+b^2}$ where a (resp. b) is the distance along the x-axis (resp. y-axis) between any two pixels of the grid.

The extraction of all foreground (resp. background) pixels that are within a distance s to the background (resp. foreground) pixels will be the basis for the characterisation of the input patterns at the size s. For conciseness, we develop our methodology for the characterisation of the foreground only. The characterisation of the background is obtained by complementing the input image and considering the dual connectivity rule.

The proposed size dependent characterisation of binary patterns and their connections is illustrated in Fig. 1 together with the individual processing steps. All steps are described in the following sections (Sections. 2.1–2.5). Note that the proposed segmentation leads to mutually exclusive categories of the foreground pixels.

2.1. Core

Core pixels are defined as those foreground pixels whose distance to the background is greater than the given size-parameter s. These pixels correspond to the erosion of the input image by a Euclidean disk of radius equal to s. They are detected by thresholding the Euclidean distance transform of the foreground for a threshold value equal to s. An exact and linear-time Euclidean distance transform algorithm is described in (Hirata, 1996), see pseudo-code in (Meijster et al., 2000).

2.2. Islet

Islet pixels are defined as those foreground connected components that do not contain any core pixel. They can be obtained by performing the difference between the input image and the reconstruction by dilation of this image using the core pixels as marker set. Fast sequential algorithms for computing reconstructions by dilation are detailed in (Vincent, 1993).

2.3. Connectors: bridge and loop

Connector pixels are groups of foreground pixels linking core connected components so that their removal would modify the homotopy of the input image. Initially, the anchored skeleton of

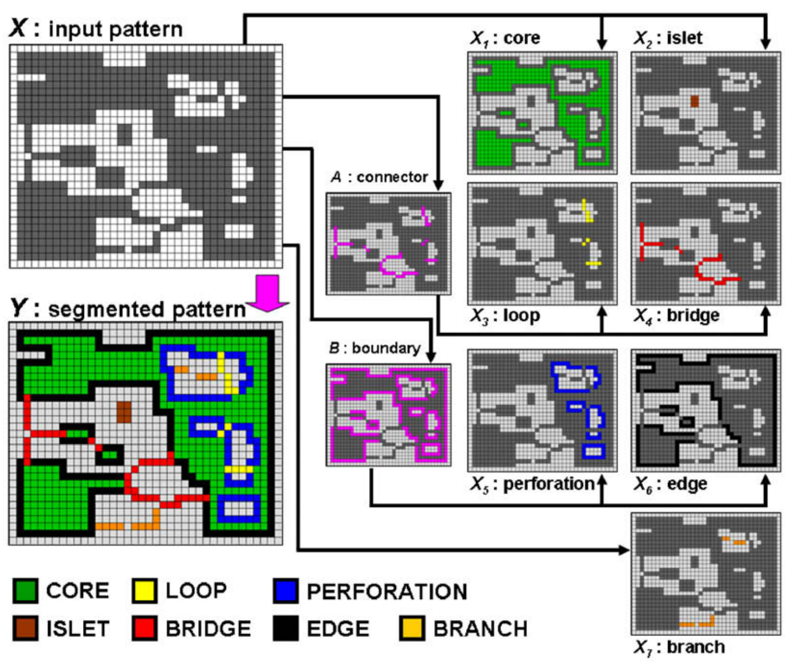

- X .... input binary image
- $X_1 = T_{d\geq s}[\mathrm{EDT}(X)]$ .... **core**
- $X_2 = X \setminus R^{\delta}_{X}(X_1)$ .... **islet**
- $A = \delta^{(s)}_{X\setminus X_1}[\mathrm{SKEL}_{X_1}(X)]$ .... connector
  - X_3 = pixels of A emanating from the same CC of X_1 .... **loop**
  - X_4 = pixels of A pixels emanating from different CCs of X_1 .... **bridge**
- $B = T_{0<d\leq s}[\mathrm{EDT}(X_1^c)] \cap [X \setminus (X_1 \cup X_2 \cup X_3 \cup X_4)]$ .... boundary
  - X_5 = pixels of B within a distance s to a hole of B .... **perforation**
  - $X_6 = B \setminus X_5$ .... **edge**
- $X_7 = X \setminus \{X_1 \cup X_2 \cup X_3 \cup X_4 \cup X_5 \cup X_6\}$ .... **branch**
- $Y = \{X_1, X_2, X_3, X_4, X_5, X_6, X_7\}$ .... segmented binary pattern

Fig. 1. Morphological segmentation of binary patterns. Top: input binary pattern X, intermediate steps X_i, and resulting segmentation Y. Bottom: successive processing steps (the name of the final seven categories are typeset in bold). T: threshold operator. EDT: Euclidean distance transform. $\setminus$: set difference. $R^{\delta}_{X}(Y)$: reconstruction by dilation of X using Y as seed. $\mathrm{SKEL}_X(Y)$: anchored skeleton of Y using X as anchor set. $\delta_X(Y)$: geodesic dilation of Y with respect to X.

the input image using the core pixels as anchor set is computed. Connector pixels are then defined as those pixels whose geodesic distance from this anchored skeleton is less than *s*, using the non-core pixels as geodesic mask. Connector pixels are themselves subdivided into two categories depending on whether the connections link the same core connected component or not:

- *bridge pixels* are connector pixels emanating from two or more core connected components;
- *loop pixels* are connector pixels emanating from the same core connected component.

The notion of anchored skeleton is detailed in (Ranwez and Soille, 2002) and fast algorithms are described in (Iwanowski and Soille, 2007).

2.4. Boundaries: edge and perforation

Boundary pixels are defined as those yet unclassified foreground pixels whose distance to the core pixels is lower than or equal to the given size-parameter *s*. They are detected by thresholding the Euclidean distance of the complement of the core pixels for all values greater than 0 and less than or equal to *s* while retaining only those yet unclassified foreground pixels.

Boundary pixels are themselves subdivided into *outer* and *inner* boundaries. For conciseness, we call the outer boundaries *edges* and inner boundaries *perforation*. Perforation pixels of a given connected component are defined as its boundary pixels that are within a distance *s* to a hole of this connected component where a hole is defined as a connected component of the background that does not contain any pixel of the border of the image. Edge pixels of this connected component are obtained by subtracting its perforation pixels from its boundary pixels.

In practice, an efficient iterative algorithm permits the distinction between perforation and edge pixels without requiring the processing of each connected component separately. The input of the algorithm is initialised with the union of core and boundary pixels. The output edge image is initialised with a void image. Then, the following three steps are applied until the input is empty:

(1) fill the holes of the input;
(2) add to the edge image the intersection between the boundaries and gradient by erosion of the filled input using a disk of radius *s* as structuring element;
(3) update the input with the foreground pixels of the current input that are embedded within its holes (i.e. intersection between the input and the filled holes of the input).

The last step of the iterative procedure is required for handling cases where a connected component of foreground pixels is itself embedded in a hole of another connected component. Once the iterative procedure terminates, the perforation pixels are obtained by subtracting the edge pixels from the boundary pixels defined at the start of this section.

2.5. Branch

Pixels that do not belong to any of the previously defined categories are called *branch pixels*. They emanate either from boundaries (edge or perforation) or connectors (bridge or loop).

Note that, connector (bridge and loop) and branch pixels that are adjacent to core pixels could be called *junction pixels* and flagged as such if required by the application.

3. Experimental results

Fig. 2 illustrates the segmentation of binary patterns on a water mask retrieved from a land cover map. In this experiment, the category core matches lakes, the category perforation islands, the category islet ponds, etc. This example emphasises that the nomenclature of the proposed seven categories correspond to actual features whose meaning is application dependent. Starting from the water mask of Fig. 2, Fig. 3 shows the proportions of each category when increasing the size-parameter. In general, the size-parameter drives the proportion of the core and non-core catego-

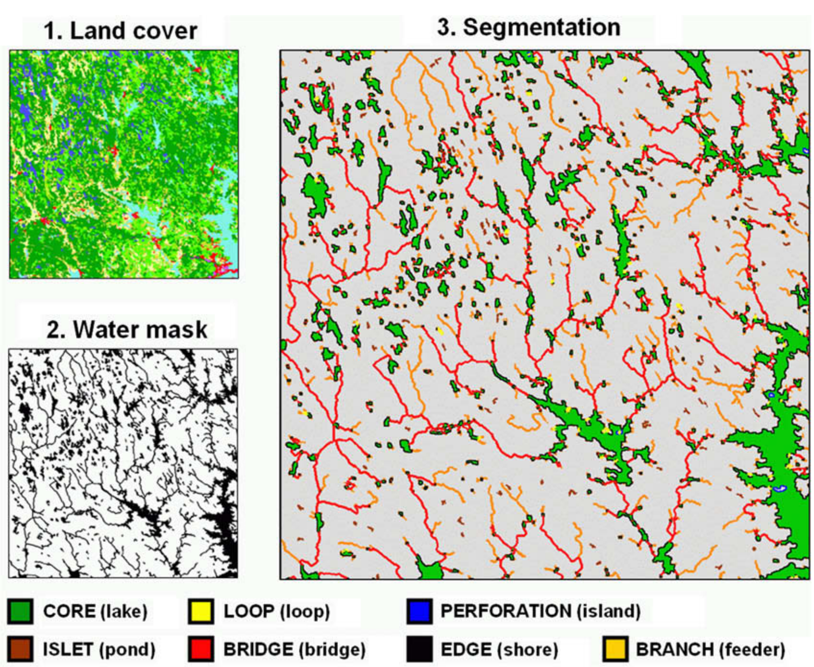

Fig. 2. Morphological segmentation of binary patterns applied to a water mask derived from a land cover map. The legend lists the generic category names with the corresponding application specific names in parenthesis.

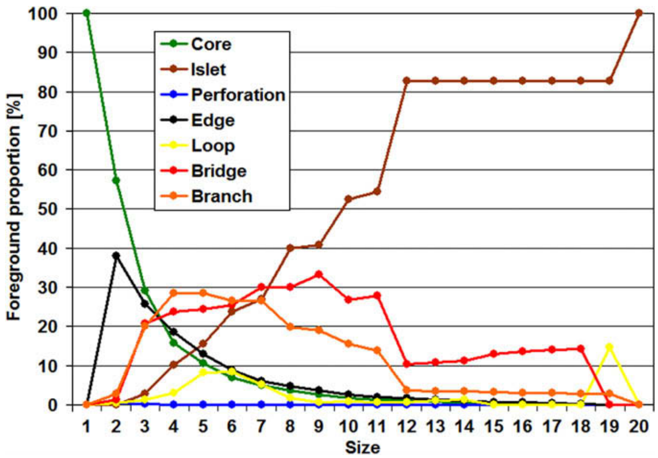

Fig. 3. Proportions of each category of the water mask of Fig. 2 for increasing size-parameter.

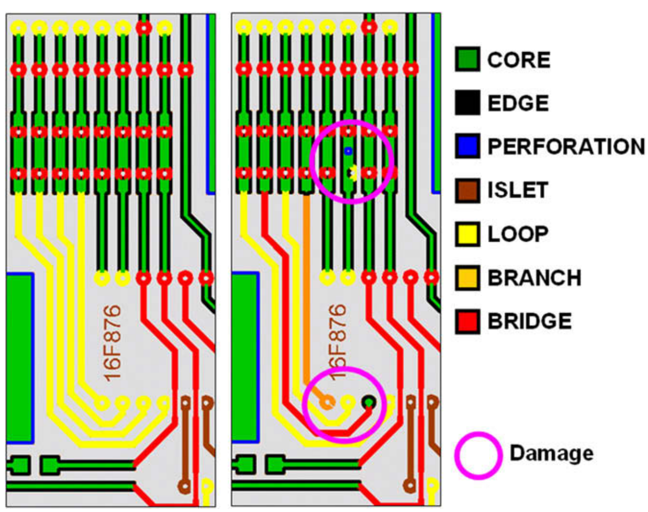

Fig. 4. Spatial pattern analysis applied to a electrical circuit board. Left: original board. Right: the same board with simulated defects (circled).

ries. Initially ($s = 0$), the entire foreground belongs to the core category. Similarly, when the value of s exceeds the maximum value of the distance transform of the image, the entire foreground belongs to the islet category. Therefore, the simultaneous existence of core and non-core categories occurs when the value of the size-parameter varies between these two boundary values. When increasing the value of the size-parameter, the core proportion always decreases while that of the islet can only increase or remain stable. By contrast, the evolution of the proportion of the remaining categories is not necessarily monotone. For these categories, fluctuations of the proportions depends on the number and distribution of the remaining core connected components. For instance, if there is only one core component, the bridge category cannot exist since the existence of the bridge category requires at least two core connected components that can be linked by a path of foreground pixels.

Fig. 4 illustrates how the segmentation algorithm could be used for quality control in manufacturing, for example a circuit board. The left panel shows the pattern of the undamaged board while the right panel illustrates the changes in segmentation categories due to simulated manufacturing errors (circle). In the upper circled area we simulated a misaligned via (hole) and a single-pixel via, both resulting in a clearly visible change of the segmentation class. The bottom circled area contains four ring structures acting as loop pathways. The simulated manufacturing error here was to open the left ring and to fill the third ring. The first error removes the loop-specific character of a ring and consequently, the class loop changes to the class branch. In the second case, when the hole is filled, the enclosed area is now large enough to contain core area and the loop has changed into a bridge between 2 core connected components.

This method was motivated by the need to describe the fragmentation of forest spatial patterns extracted from satellite images, see Vogt et al. (2007) for preliminary results with emphasis on the application. Any test image can be processed using the free software package GUIDOS available at the following URL: http://forest.jrc.ec.europa.eu/biodiversity/GUIDOS/.

4. Concluding remarks

The proposed method and algorithms allow for a generic segmentation of binary patterns into categories representing specific geometric features. The method is generic in the sense that it can be applied to any binary patterns. The extension of the proposed method to 3-D images would need adaptations to take into account the distinction between surfacic and curvilinear 3-D objects. This could be of interest for future research and particularly for 3-D medical images. Finally, rather than considering binary patterns, it would be interesting to generalise the methodology to partitions of the space for more than two classes (background and foreground). This could be achieved using concepts related to generalised geodesic transformations (Soille, 1994).

References

Beisbart, C., Buchert, T., Wagner, H., 2001. Morphometry of spatial patterns. Physica A 293, 592–604.
Hirata, T., 1996. A unified linear-time algorithm for computing distance maps. Inform. Process. Lett. 58 (3), 129–133.
Iwanowski, M., Soille, P., 2007. Fast algorithms for order independent binary homotopic thinning. Lect. Notes Comput. Sci. 4432 (2), 606–615. doi:10.1007/978-3-540-71629-7_68.
Meijster, A., Roerdink, J., Hesselink, W., 2000. A general algorithm for computing distance transforms in linear time. In: Goutsias, J., Vincent, L., Bloomberg, D. (Eds.), Mathematical Morphology and its Applications to Image and Signal Processing, Volume 18 of Computational Imaging and Vision, Boston. Proc. of ISMM'2000, Palo Alto, June 26–29. Kluwer Academic Publishers, pp. 331–340. <http://oldwww.rug.nl/hpc/people/arnold/articles/ismm2000.pdf>.
Ranwez, V., Soille, P., 2002. Order independent homotopic thinning for binary and grey tone anchored skeletons. Pattern Recognition Lett. 23 (6), 687–702. doi:10.1016/S0167-8655(01)00146-5.
Serra, J., 1982. Image Analysis and Mathematical Morphology. Academic Press, London.
Soille, P., 1994. Generalized geodesy via geodesic time. Pattern Recognition Lett. 15 (12), 1235–1240. doi:10.1016/0167-8655(94)90113-9.
Soille, P., 2003. Morphological Image Analysis: Principles and Applications, second ed. Springer-Verlag, Berlin/Heidelberg/New York.
Vincent, L., 1993. Morphological grayscale reconstruction in image analysis: Applications and efficient algorithms. IEEE Trans. Image Process. 2 (2), 176–201.
Vincent, L., Soille, P., 1991. Watersheds in digital spaces: An efficient algorithm based on immersion simulations. IEEE Trans. Pattern Anal. Machine Intell. 13 (6), 583–598. doi:10.1109/34.87344.
Vogt, P., Riitters, K., Iwanowski, M., Estreguil, C., Kozak, J., Soille, P., 2007. Mapping landscape corridors. Ecological Indicators 7 (2), 481–488. doi:10.1016/j.ecolind.2006.11.001.